Nuclear Inst. and Methods in Physics Research, A 1049 (2023) 168094

Contents lists available at ScienceDirect

Nuclear Inst. and Methods in Physics Research, A

journal homepage: www.elsevier.com/locate/nima

Full Length Article

Design of the proton and electron transfer lines for AWAKE Run 2c

R. Ramjiawan [a,*], V. Bencini [b,a], P.N. Burrows [b], F.M. Velotti [a]

[a] CERN, CH-1211, Geneva, Switzerland

[b] John Adams Institute for Accelerator Science, University of Oxford, Oxford, United Kingdom

ARTICLE INFO

Keywords:
Plasma wakefield acceleration
Transfer lines
Numerical optimisation
Beam dynamics

ABSTRACT

The Advanced Wakefield (AWAKE) Run 1 experiment, which concluded in 2018, achieved electron acceleration to 2 GeV via plasma wakefield acceleration driven by 400 GeV, self-modulated proton bunches extracted from the CERN SPS. The Run 2c phase of the experiment aims to advance these results by demonstrating acceleration up to about 10 GeV while preserving the quality of the accelerated electron beam. For Run 2c, the Run 1 proton transfer line will be reconfigured to shift the first plasma cell 40 m longitudinally and a second plasma cell will be added 1 m downstream of the first. In addition, a new 150 MeV beamline will be required to inject a witness electron beam, with a beam size of several microns, into the second plasma cell to probe the accelerating fields. Proposed adjustments to the proton transfer line and the design of the 150 MeV electron transfer line are detailed in this paper.

1. Introduction

1.1. AWAKE Run 1

Run 1 of the AWAKE Experiment demonstrated the acceleration of electron beams to GeV-energies via proton-driven plasma wakefield acceleration [1,2]. The Run 1 plasma cell was a 10-m-long Rubidium vapour cell within which a plasma channel of radius 1 mm was produced via the ionisation of Rubidium gas with a high-power laser pulse [3]. The wakefield driver, a 400 GeV proton beam extracted from the CERN Super Proton Synchrotron (SPS), was injected into the plasma where the 12-cm-long bunch underwent self-modulation to produce a train of micro-bunches with lengths of approximately half of the $O(1\,\mathrm{mm})$ plasma wavelength [4,5]. These trains of micro-bunches resonantly drove wakefields within the plasma which were probed by 18.84 MeV witness electron bunches [1]. The laser pulse which ionised the Rubidium gas co-propagated in the plasma with the proton beam and caused a relativistic ionisation front which was used to seed the self-modulation of the proton bunch behind the laser pulse.

The witness electron beams were produced with an S-band, RF photo-cathode gun and accelerated in a travelling-wave booster linac to 16–20 MeV [6]. A transfer line [7], with both horizontal and vertical bends, transported the electron beams for injection into the plasma cell with a beam size of $\sigma = 250\,\mu\mathrm{m}$. The injected electron beams propagated co-linearly in the plasma with the proton and laser beams. Injected electrons which were captured within the focusing, accelerating phase of the plasma wakefields were accelerated and could be used to measure the accelerating gradient. With the nominal plasma electron density, $7 \times 10^{14}\ \mathrm{cm}^{-3}$, it was estimated that average accelerating gradients of 200 MV/m were achieved [8].

1.2. AWAKE Run 2

The aim of AWAKE Run 2 is to improve the energy reach compared with Run 1 while preserving a smaller emittance and energy spread to produce a beam suitable for high-energy physics applications [10]. Run 2 is planned to comprise four stages [11]. Run 2a studies the seeding of the proton bunch self-modulation with a ∼18 MeV electron bunch to ensure the self-modulation of the full proton bunch is phase-stable and reproducible [12]. During Run 2b, a density step will be introduced in the plasma to stabilise the self-modulation process [13]. The aim for Run 2c is to achieve electron energies up to 10 GeV with a smaller emittance and energy spread than Run 1. To achieve this, the proton bunch self-modulation and the electron bunch acceleration will be separated between two plasma cells to prevent the emittance growth of the electron bunch which would occur if exposed to the defocusing fields of the un-modulated proton bunch [14]. A schematic of the proposed Run 2c beamline configuration is shown in Fig. 1. The aim of Run 2d will be to demonstrate the scalability of the acceleration method to longer plasma cells and thus higher energies.

For Run 2c, a seeding electron beamline will be used to inject electron bunches into the first plasma cell to seed the proton bunch self-modulation. To incorporate a seeding electron beamline and second plasma cell, the first plasma cell will be shifted 40 m downstream, requiring reconfiguration of the proton beamline. To limit the defocusing of the proton beam between the two plasma cells the gap between

* Corresponding author.
E-mail address: rebecca.louise.ramjiawan@cern.ch (R. Ramjiawan).

https://doi.org/10.1016/j.nima.2023.168094
Received 21 October 2022; Received in revised form 10 January 2023; Accepted 25 January 2023
Available online 30 January 2023
0168-9002/

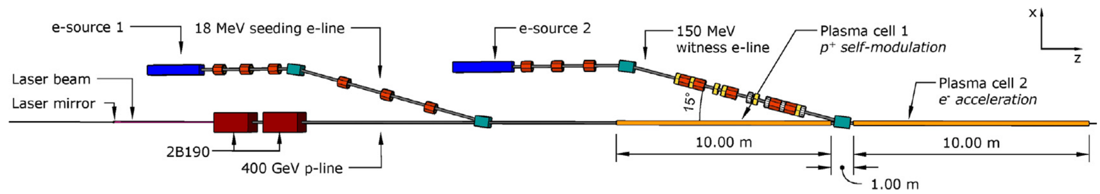

Fig. 1. Schematic of the configuration of the seeding and witness electron beamlines, plasma cells and final section of the proton transfer line; with dipoles (cyan), quadrupoles (red), sextupoles (yellow) and octupoles (white) [9].

Table 1
Beam parameters for the AWAKE Run 2c proton and witness electron transfer lines [10].

Parameter		p^+-line	e^--line
Beam energy	E	400 GeV	150 MeV
Charge	q	48 nC	100–200 pC
Bunch length	σ_z	6–12 cm	60 μm
Momentum spread	$\delta p/p$	0.03%	0.2%
Norm. emittance	ϵ	3.5 mm mrad	2 mm mrad

Table 2
AWAKE Run 2c proton transfer line experimental specifications at the injection point compared with the parameters of the proposed design [19].

Parameter	Units	Design	Specification
β_x	[m]	4.9	4.9
β_y	[m]	4.9	4.9
α_x	[rad]	0.0	0.0
α_y	[rad]	0.0	0.0
D_x	[m]	0.0	0.0
D_y	[m]	0.04	0.0
σ_x	[μm]	200.6	200(20)
σ_y	[μm]	200.1	200(20)

them should be less than 1 m [15]: the witness electron beam will be injected into the second plasma cell from within this gap. To minimise the emittance growth during acceleration, the injected witness electron beam parameters must be carefully chosen, as described in Section 3.1 [16,17]. The parameters for the Run 2c seeding electron line will be determined from the results of the Run 2a studies and it is expected to reuse elements from the Run 1 electron beamline.

In this paper, we present proposals for the design of the witness electron line and the reconfiguration of the proton line; beam parameters for these lines are given in Table 1. The design of the transfer line was performed using MAD-X [18].

2. Proton transfer line

2.1. Transfer line reconfiguration

The Run 1 proton transfer line was adapted from the previous CERN Neutrinos to Gran Sasso (CNGS) line. During the conversion to the AWAKE experiment, a laser line was added to provide the laser beam to ionise the Rubidium gas. A laser mirror was installed, upstream of the plasma cell, to merge this laser beam onto the axis of the proton beam. To incorporate this mirror, a half-chicane was added to the proton line to avoid the intersection of the high-energy proton beam and mirror as this would cause losses of the proton beam and produce radiation. The half-chicane was constructed by moving the final dipole, MBG.412115 (Fig. 2(a)), downstream and adding two pairs of B190 dipoles to bend the proton beam onto the axis of the plasma cell.

After extending the Run 2c proton line by 40 m, it should be reconfigured and re-matched to achieve the same beam parameters at injection into the first plasma cell as for Run 1 (Table 2) [19]. Due to limitations from the power converters, the Run 2c design should not include any additional magnets. To preserve the laser beam stability of Run 1, the merging-mirror should be moved downstream with the plasma cell, requiring the half-chicane to be widened and lengthened. The proposed Run 2c proton-line layout is compared with the Run 1 layout in Fig. 2(a). The dipole MBG.412115 was moved an additional 12.5 m downstream, widening the half-chicane from 8 cm to 18 cm [19]. If the start and end of the half-chicane were also shifted 20 m and 40 m, respectively, it would allow the laser mirror to be moved 35 m from the Run 1 location, as shown in Fig. 2(a) [19]. This would mean a distance of 26 m between the laser merging-mirror and the plasma injection point, compared with 21 m for Run 1.

This design satisfies the experimental specifications, as shown in Table 2. The beam optics are presented in Fig. 3, where the beam envelope ($6\sigma_{x,y}$) includes an orbit error of $2\,\text{mm} \times \sqrt{\frac{\beta_{\text{local}}}{\beta_{\text{max.}}}}$, a 2 mm alignment error and +20% error in $\beta_{x,y}$. This design would provide a 2 mm clearance between the beam envelope and the laser-merging mirror (Fig. 2(b)). For comparison, Run 1 had a 5.6 mm clearance between the beam envelope and the mirror. By extending the line by 40 m without additional magnets, the beam envelope would be close to the apertures, particularly within the half-chicane.

2.2. Beam accuracy and stability

For a plasma density of 7×10^{14} cm^{-3}, an offset of more than 13 μm between the driver and witness beams would lead to an unacceptable emittance growth during acceleration [16]. The relative offset between the two beams comprises both the static offset between beams and their respective jitters and therefore, ideally, the r.m.s jitters of the respective beams should be kept below 2 μm. With a higher beam jitter, fewer shots will be suitable for the experiment leading to poorer efficiency.

The proton beam pointing accuracy should be sufficient to have overlap between the proton beam and laser beam through the full length of both plasma cells. If the Run 1 instrumentation was reused, the alignment of the proton beam could be measured with beam position monitors (BPMs) of resolution 50 μm located 1.7 m upstream of the first plasma cell and 22.9 m downstream of the second plasma cell. With interpolation to the plasma cell entrance, this would correspond to a single-shot resolution of 47 μm in position and 4 μrad in angle. The resolution could be improved by taking several shots and averaging the results. The final correctors to steer the beam through the plasma cell are 9 m from the injection point of the first plasma cell, as for Run 1.

Two of the dominant sources of shot-to-shot proton beam jitter at the injection point are the current jitter of the SPS extraction septum, MSE.4, and ripples on the power converters for the magnets in the proton line (TT40/TT41). The power converter jitter would primarily cause horizontal transverse jitter at the merge-point because the bending occurs in this plane. The MSE.4 current jitter causes horizontal angular jitter of the beam at the start of the TT40 line. The magnitude of these effects was calculated from data recorded in June 2020 and was propagated using the Run 2c optics model (Fig. 3) to the injection point. The measured current jitters and their simulated impact on the proton beam position reproducibility at injection are given in Table 3. The MSE.4 current jitter corresponded to 1.4 μrad angular jitter.

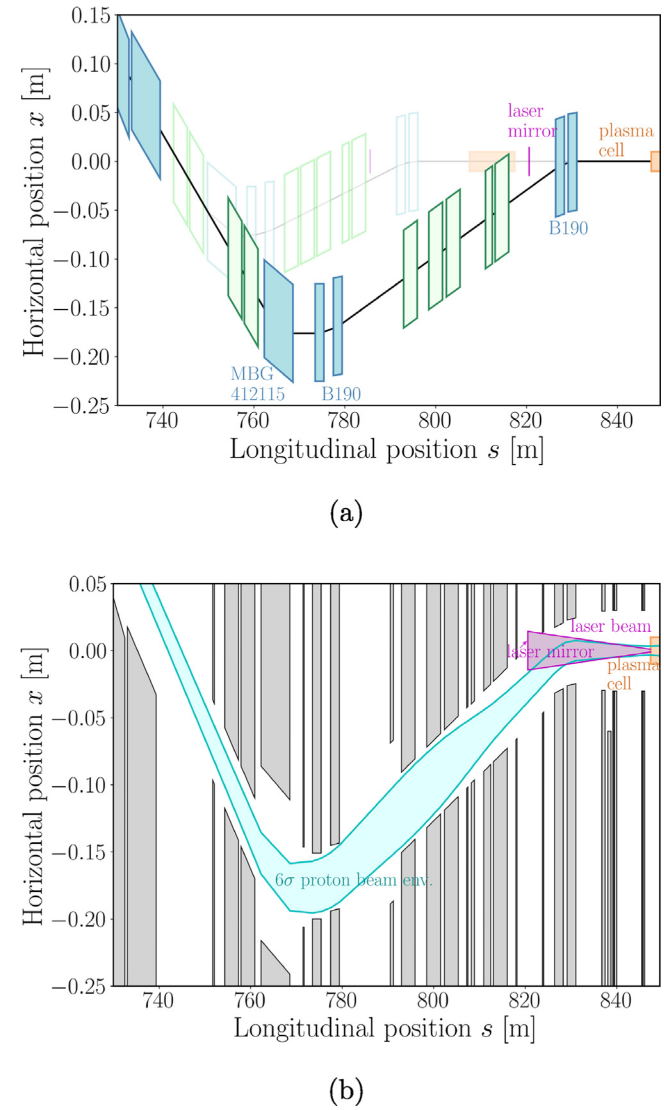

Fig. 2. (a) Reconfiguration of the chicane layout showing the Run 1 (translucent) and Run 2c (bold) chicanes, (b) $6\sigma_x$ beam envelopes for Run 2c, as defined in the text, with horizontal magnet apertures shown in grey. The location of the laser-merging mirror is indicated [19].

Table 3
Measured magnet current jitter and corresponding beam position jitter propagated to the injection point with Run 2c optics. The range of quadrupole jitters refers to the spread across different quadrupole families. Here, only magnet current errors were included (without magnet offsets), so the position jitter caused by quadrupole current jitter could not be meaningfully estimated.

Magnet class	Current r.m.s jitter (ppm)	Beam r.m.s jitter (μm)	
		x	y
B190	50	6.9	0.0
MBG	90	71.5	10.5
MBHC	100	22.0	0.0
Quadrupole	50–200	–	–
MSE.4	100	28.8	0.0

To perform a more complete study of the impact of errors on the beam stability, the beam transport was simulated with all of the current jitters shown in Table 3 as well as magnet misalignments and rotations. The magnet misalignments and rotations were randomly sampled from Gaussian distributions with standard deviations of 100 μm and 400 μrad,

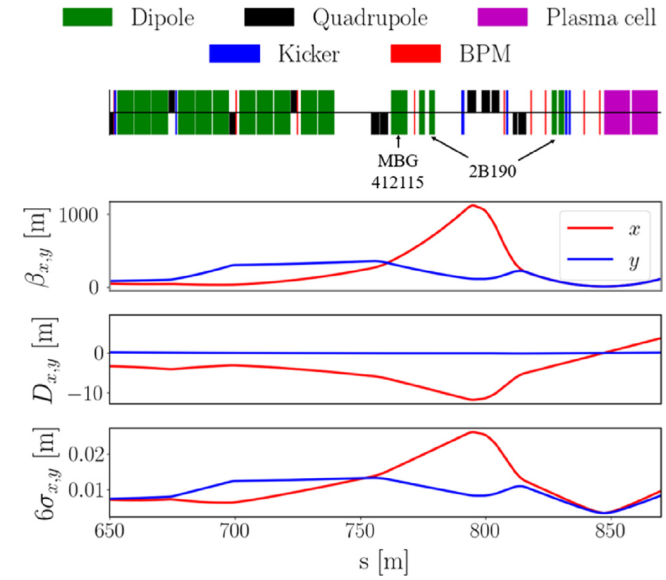

Fig. 3. MAD-X simulation of the proposed Run 2c proton transfer line, showing horizontal and vertical β-functions, dispersions and 6σ beam envelopes, as defined in the text [19].

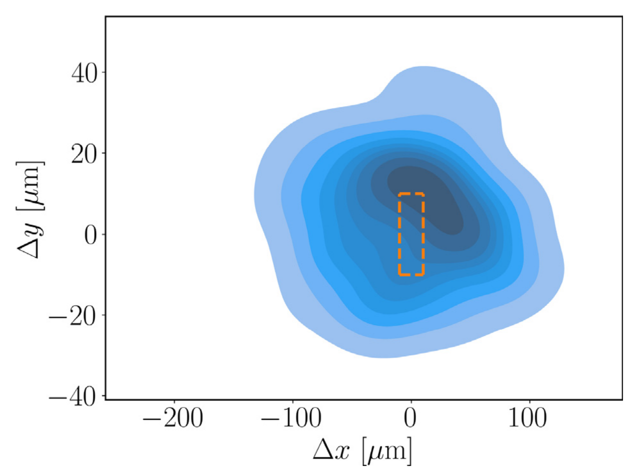

Fig. 4. Distributions of relative driver-witness offsets at the injection-point for 100 seeds after beam-based alignment of the witness electron beam [9]. The orange lines denote the experimental specification.

respectively. The simulated r.m.s position jitter at the injection point of the first plasma cell was 42 ± 3 μm horizontally and 3.9 ± 0.3 μm vertically. This is consistent with measured data from Run 1 which showed that the 1σ jitter of the bunch at the beam-waist position was 41 μm horizontally and 8 μm vertically, after drift correction [20].

The simulated beam jitter at the second plasma cell is 82 ± 6 μm horizontally and 10.5 ± 0.7 μm vertically, meaning that only 6% of shots would satisfy the experimental tolerances for the driver-witness beam misalignment (Fig. 4). The efficiency of the AWAKE Run 2c experiment could be improved by upgrading the TT40/TT41 power converters. These power converters are foreseen to be upgraded to the LHC Class 3 power converters [21] during the CERN Long Shutdown 3, meaning that 15% of shots could be within the alignment tolerance. This efficiency would be sufficient for the experiment. If, additionally, the MSE.4 were upgraded to Class 3 then up to 33% of shots would be suitable.

3. Electron 150 MeV witness transfer line

3.1. Transfer line specification

For Run 2c, a new transfer line will be added to inject 150 MeV witness electron bunches into the second plasma cell. The beam energy was selected to be high enough to avoid space-charge effects but low enough to use only a single klystron. A dog-leg design with 15° bends was chosen, where the dipole placements and bending angle were selected based on spatial constraints from the tunnel width and the arrangement of the two plasma cells (Fig. 1) [19]. The electron source is expected to be on the same horizontal plane and vertical inclination as the proton line.

The injected witness bunch should have a length of $\sigma_z \approx 60\,\mu\text{m}$, so as to be within a regime of optimal beam loading and thus maintain a small energy spread during acceleration [17,22]. To preserve a small emittance throughout acceleration, there should be sufficient charge density in the witness bunch to drive a full blow-out of the electrons remaining in the plasma wakefield bubble. The bunch should also be matched to the plasma wakefield bubble to prevent oscillations of the witness bunch in the plasma which could cause emittance growth. The matched beam size is [17]

$$\sigma^* = \sqrt[4]{\frac{2\varepsilon_0 m_e c^2 \gamma}{n_{pe} e^2}\epsilon^2} = 5.75\,\mu\text{m}, \tag{1}$$

where the Lorentz factor $\gamma = 293.5$, m_e is the mass of an electron, c is the vacuum speed of light, ε_0 is the vacuum permittivity, e is the electron charge, the normalised emittance $\epsilon = 2$ mm mrad and the plasma density n_{pe} has baseline values: 2×10^{14} cm^{-3} or 7×10^{14} cm^{-3}. In this paper we focus on the more challenging 7×10^{14} cm^{-3} plasma density. Although, ideally, the witness beam would be properly matched to the plasma, if this is not possible, the witness beam size must remain below 1.5 times the matched beam size to keep emittance growth within acceptable limits [16]. The beam profile should be Gaussian in six dimensions (x, p_x, y, p_y, z, p_z).

3.2. Transfer line design

Here we describe the baseline witness transfer line design and show that it satisfies experimental specifications and spatial constraints. The requirements for the line were challenging and the use of numerical optimisers in the design process was crucial [9]. To study the higher order effects, beam tracking studies were performed using a MAD-X implementation of PTC [23]. As an input to tracking simulations, a beam distribution was produced from simulations of the electron gun and adjusted to have Gaussian x, y, p_x, p_y profiles, this is shown in Fig. 5. The $E - z$ distribution from the electron gun was preserved and scaled to have the nominal 0.2% momentum spread.

A triplet of quadrupoles before the first dipole provide the primary control for the focusing of the line. Five quadrupoles between the dipoles are used to make the dog-leg achromatic and provide additional focusing (Fig. 6). For a dog-leg with only two dipoles, there is no independent control to make the line both achromatic and isochronous. To inject a bunch with a length of 60 μm at the injection point, the line was designed to have a shortening effect on the bunch, to be counter-acted by injecting a bunch which is 40% longer into the line [19]. The beam optics are presented in Fig. 6 and the simulated injection-point parameters are given in Table 4.

To achieve a compact design with a small beam size at injection, strong focusing was required, leading to problematic non-linear effects including betatron chromatic effects and detuning with amplitude. In order to keep these unwanted terms under control, sextupoles and octupoles were required. The footprint of the proposed design is presented in Fig. 7, showing the locations of all magnets. The apertures were modelled as ±25 mm and the two high-beta regions within the dog-leg

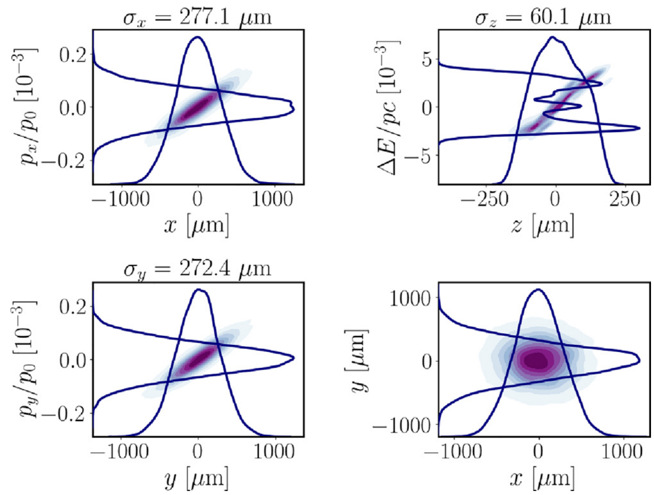

Fig. 5. Generated input beam distribution of 100 000 macro-particles with $\beta_{x,y} = 11$ m, $\alpha_{x,y} = -2.1$ and $\epsilon_{x,y} = 2$ mm mrad.

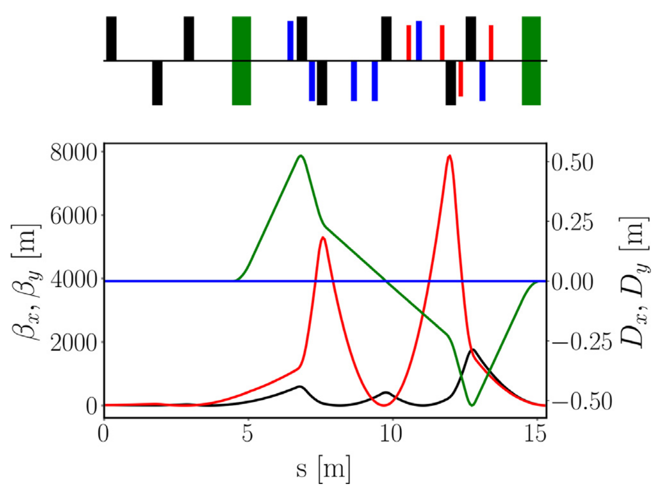

Fig. 6. Beam parameters for the 150 MeV electron transfer line, with β-function (x: black, y: red) and dispersion D (x: green, y: blue). A synoptic overview is given above, with dipoles (green), quadrupoles (black), sextupoles (blue) and octupoles (red).

Table 4
Run 2c witness electron transfer line Twiss parameters (β, α), beam size ($\sigma_{x,y}$), bunch length (σ_z) and dispersion (D) at the injection point of the second plasma cell.

Parameter	Units	Specification	Design
β_x/β_y	[mm]	4.9	4.8/5.4
α_x/α_y	[mm]	0.0	0.0/0.0
D_x/D_y	[m]	0.0	0.0/0.0
σ_x/σ_y	[μm]	5.75	6.0/6.1
σ_z	[μm]	60	59.9

(Fig. 6) mean that the beam envelope is close to the aperture limits and the transfer line would not be suitable for a higher emittance beam.

The input bunch distribution (Fig. 5) was tracked through the transfer line to the injection point, resulting in the beam distribution presented in Fig. 8. Even when including non-linear effects, the beam size is within the tolerance for the experimental specification. These results are for an ideal beamline and in Section 3.3 we consider the impact of errors on achieving a matched beam.

3.3. Errors and misalignments

In this section we consider the impact of a range of error sources on the beam size and alignment at the injection point. Studies of each

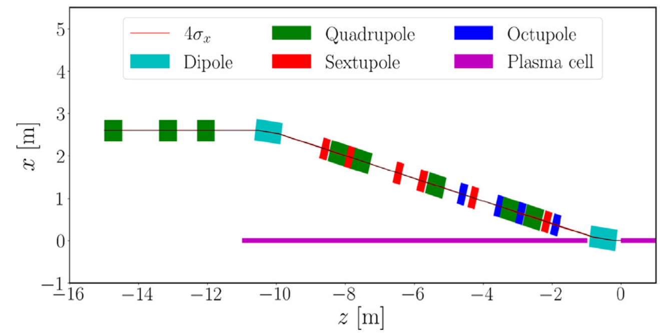

Fig. 7. Footprint of the proposed witness electron transfer line with estimated element sizes; σ_x is the horizontal beam size [19].

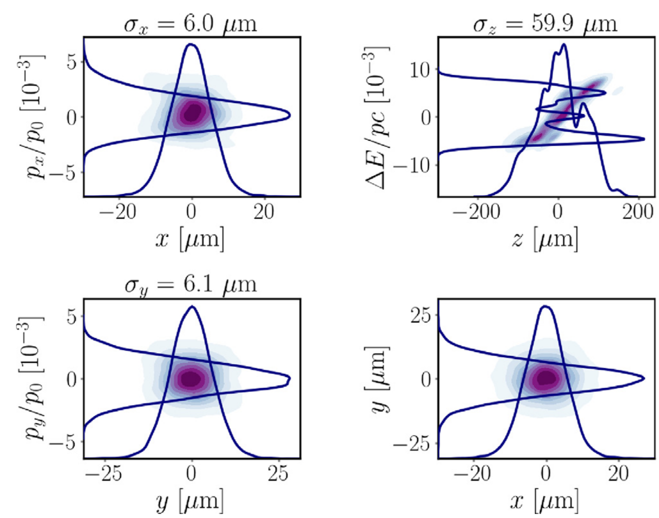

Fig. 8. Beam distributions and profiles for a beam with normalised emittance 2 mm mrad and length σ_z = 84 μm tracked to the injection point. The structure in the $z - \Delta E/pc$ distribution originates from the input distribution.

error source were performed individually to isolate their effects. This was then used to specify upper bounds on their tolerances.

Starting from an ideal beamline, quadrupole misalignments were applied, sampled randomly from a Gaussian distribution; beam tracking was then used to determine the resulting injection-point beam size. The results of this are shown in Fig. 9(a) as a function of the standard deviation of the distribution of errors used. This study determined that, through beam-based alignment (BBA) and steering, a quadrupole alignment of better than 7 μm with the beam should be attained. To achieve this level of magnet-beam alignment, the magnets would need to be on movers with a step size of approximately 1 μm and with a range of 100 s of microns. A proposal for the quadrupole alignment process is detailed in [9]. The alignment process includes 'quadrupole shunting' to align the quadrupoles with the beam and 'dispersion-free steering' to minimise residual dispersion caused by offset magnets. The assumed BPM and beam screen (BTV) locations for the BBA are shown in Fig. 10. The BPMs were modelled with a resolution of 10 μm, and the injection-point BTV was modelled with a position resolution of 10 μm and a beam size resolution of 1 μm.

The corresponding studies for the sextupoles and octupoles are presented in Fig. 9(b) showing that the BBA should reach an alignment of better than 20 μm for the sextupoles and better than 25 μm for the octupoles. This alignment is foreseen to be achieved using a numerical optimiser which would vary the sextupole and octupole mover positions based on minimising the beam size at the injection-point BTV. In [9], the BOBYQA [24] algorithm was found to be suitable for this alignment method.

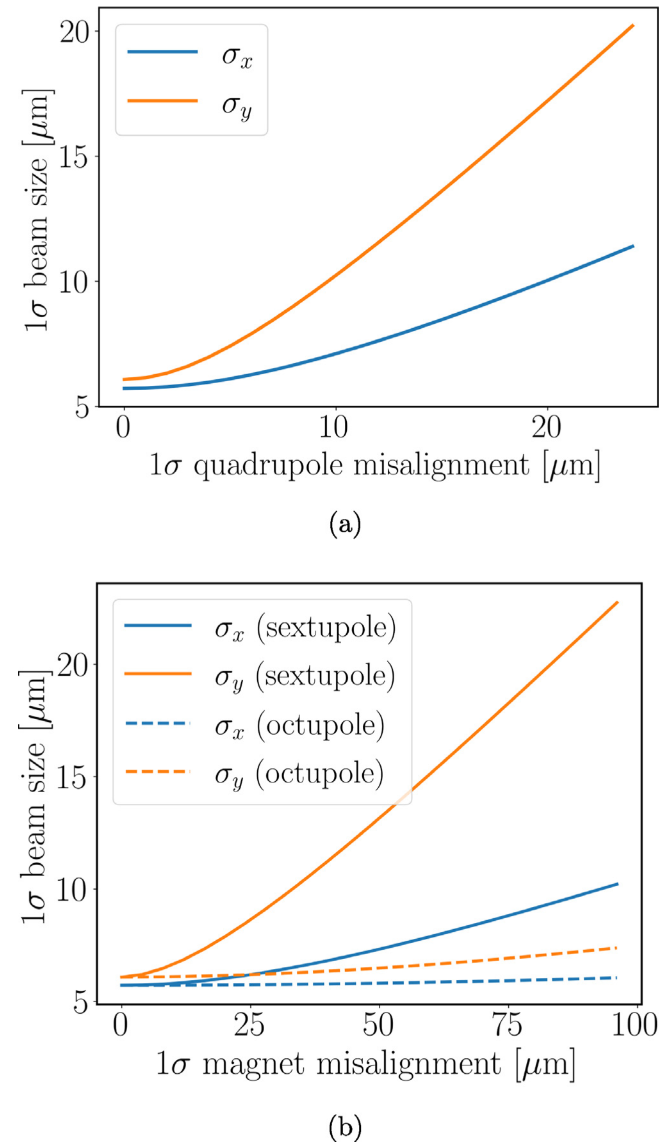

Fig. 9. Horizontal and vertical injection-point beam sizes averaged over 50 seeds with (a) quadrupole and (b) sextupole and octupole misalignments sampled randomly from a Gaussian distribution with standard deviation given by the x-axis.

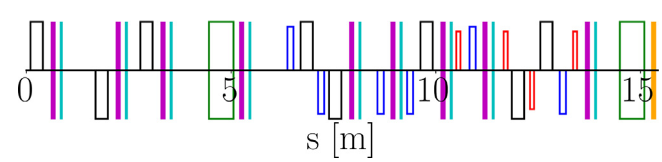

Fig. 10. Schematic showing the locations of BPMs (cyan), a BTV (yellow) and correctors (purple). Magnet positions are shown as outlines. The beam goes from left to right.

Using full error simulations we have found that, with the alignment techniques discussed above, it may be possible to achieve 85% of shots within the experimental beam size tolerances (Fig. 11).

3.4. Coherent Synchrotron Radiation

To study whether this transfer line would produce significant effects from Coherent Synchrotron Radiation (CSR), beam tracking was performed using the simulation framework Ocelot [25]. The bunch

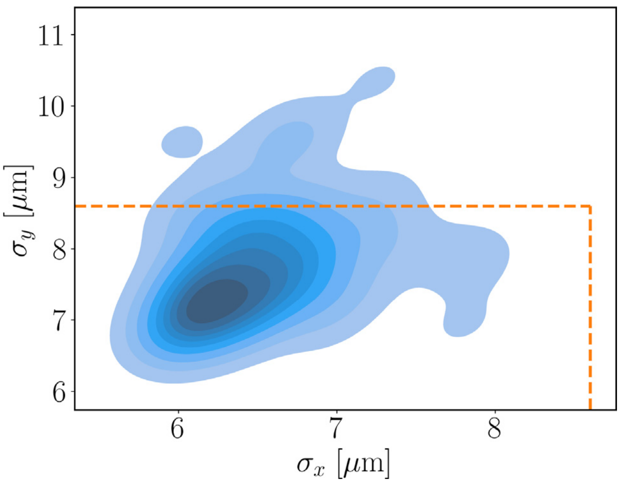

Fig. 11. Distributions of beam sizes at the injection-point for 100 seeds with errors as described in Section 3.3 and after beam-based alignment [9]. The orange lines denote the experimental specification.

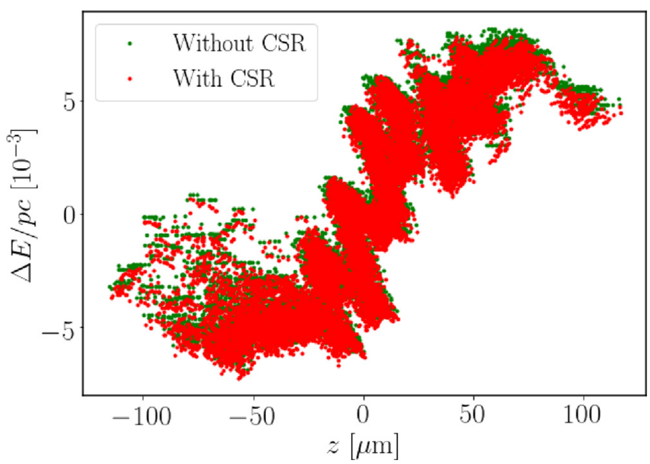

Fig. 12. Distribution of energy vs. longitudinal position for a bunch tracked to the injection point using Ocelot both with and without including CSR effects.

distribution was tracked to the injection point both with and without CSR, this is shown in Fig. 12. The inclusion of CSR effects caused a 3% shift in energy and a 6 μm offset in beam centroid position. The impact from CSR effects is approximately 25% from the first dipole and 75% from the second dipole. To account for the energy and position shift, the dog-leg should be re-matched for the new energy and the beamline adjusted to counteract the static position offset.

3.5. Scattering foils

The AWAKE experiment will incorporate two thin foils in the beamline just upstream of the focal point, one as the plasma cell vacuum window and the other as the beam dump for the ionising laser [26]. The configuration of the two foils is shown in Fig. 13. As a result of the energy of the beam relative to the radiation length and thickness of the foil, the main driver to the change of emittance and optics is Multiple Coulomb Scattering (MCS). From the MCS, the angular dispersion is [27]

$$\theta_0 = \frac{13.6}{\beta c p} z \sqrt{\frac{t_0}{X_0}}[1 + 0.038 \ln \frac{t_0}{X_0}], \tag{2}$$

with c the vacuum speed of light, $\beta = \frac{v}{c}$, p the momentum in MeV/c, X_0 the radiation length of the foil material and t_0 the foil thickness. Both

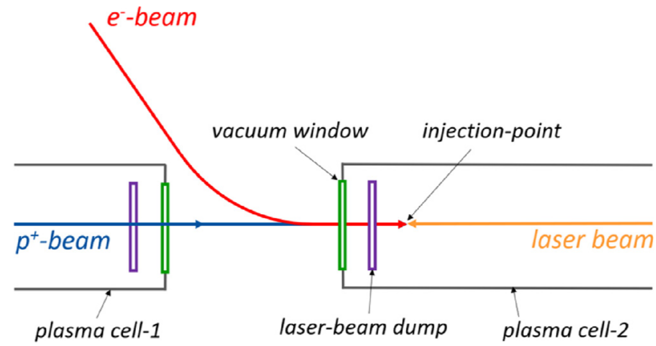

Fig. 13. Schematic of the witness electron injection region highlighting the locations of the vacuum window and laser-beam dump.

foils were modelled as aluminium foils with t_0 = 100 μm, X_0 = 8.9 cm and 1 mm separation both between the two foils and between the final foil and the injection point.

The beam scattering in the foil increases the emittance by an amount which is dependent on the beta function at the foil [28]. The beta function after the foil is consequently reduced, thus requiring the optics to be re-optimised to return the beam focal point to the injection point. With the increased emittance, the beam sizes were 17.2 μm and 17.6 μm horizontally and vertically, which were both within 5% of the matched beam sizes.

4. Conclusion

In this paper we have presented the current baseline designs for the Run 2c proton and electron transfer lines. For Run 2c, the AWAKE experiment will be adapted to achieve a higher energy and an improved beam quality compared with Run 1. The proton transfer line will need extending by 40 m while maintaining the same beam parameters at the plasma entrance as for Run 1. A new 150 MeV electron beamline will be added to inject witness electron bunches into the second plasma cell, and a lower energy beamline will inject electron bunches into the first plasma cell to seed the proton bunch self-modulation.

Adjustments to the proton transfer line were described, showing that the transfer line could be extended by 40 m without additional magnets. The precise alignment between the driver and witness beams is essential for Run 2c, and simulations of the expected Run 2c stability with the current equipment were presented. Ideally, the proton and electron r.m.s beam jitters would each be below 2 μm. The results showed that without an upgrade of the power converters only 6% of shots would satisfy experimental requirements.

The baseline design for the 150 MeV witness electron transfer line was presented. The design would use a dog-leg shape to satisfy spatial constraints in order to inject bunches into the second plasma cell from within the 1-m-gap between two plasma cells. The tight spatial constraints and strict tolerances on beam size and stability meant that this was a challenging transfer line to design. The transfer line design meets the requirements for beam size and stability so as to match the beam to the plasma and maintain a low emittance and energy spread during acceleration. Studies of the impacts of a range of errors and misalignments were discussed, demonstrating the importance of minimising the magnet misalignments through beam-based alignment to maximise the experiment efficiency.

Declaration of competing interest

The authors declare the following financial interests/personal relationships which may be considered as potential competing interests: Rebecca Ramjiawan reports financial support was provided by Science and Technology Facilities Council.

Data availability

Data will be made available on request.

Acknowledgements

We thank S. Döbert, J. Farmer, V. Fedosseev, E. Gschwendtner, G. Le Godec, S. Mazzoni, P. Muggli, L. Verra and G. Zevi Della Porta for helpful discussions. We are grateful for the financial support of this research from the Science and Technology Facilities Council (AWAKE-UK, Cockcroft Institute core, John Adams Institute core, and UCL consolidated grants), United Kingdom.

References

[1] E. Adli, et al., (AWAKE Collaboration), Acceleration of electrons in the plasma wakefield of a proton bunch, Nature 561 (7723) (2018) 363–367.

[2] E. Gschwendtner, et al., (AWAKE Collaboration), AWAKE, the advanced proton driven plasma wakefield acceleration experiment at CERN, Nucl. Instrum. Methods A 829 (2016) 76–82.

[3] E. Öz, P. Muggli, A novel Rb vapor plasma source for plasma wakefield accelerators, Nucl. Instrum. Methods A 740 (2014) 197–202.

[4] E. Adli, et al., (AWAKE Collaboration), Experimental observation of proton bunch modulation in a plasma at varying plasma densities, Phys. Rev. Lett. 122 (5) (2019) 054802.

[5] M. Turner, et al., (AWAKE Collaboration), Experimental observation of plasma wakefield growth driven by the seeded self-modulation of a proton bunch, Phys. Rev. Lett. 122 (5) (2019) 054801.

[6] S.-Y. Kim, S. Doebert, O. Apsimon, R. Apsimon, G. Burt, M. Dayyani, S. Gessner, I. Gorgisyan, E. Granados, S. Mazzoni, et al., Commissioning of the electron injector for the AWAKE experiment, Nucl. Instrum. Methods A 953 (2020) 163194.

[7] J. Schmidt, O.R. Jones, P. Muggli, M. Fraser, L. Jensen, B. Biskup, E. Gschwendtner, E. Bravin, A. Vorozhtsov, C. Bracco, et al., The AWAKE electron primary beam line, in: Proc. of IPAC '15, Richmond, VA, USA, 2015.

[8] K. Lotov, V. Minakov, A. Sosedkin, Parameter sensitivity of plasma wakefields driven by self-modulating proton beams, Phys. Plasmas 21 (8) (2014) 083107.

[9] R. Ramjiawan, S. Döbert, J. Farmer, E. Gschwendtner, F.M. Velotti, L. Verra, G.Z. Della Porta, V. Bencini, P.N. Burrows, Design and operation of transfer lines for plasma wakefield accelerators using numerical optimizers, Phys. Rev. Accel. Beams 25 (2022) 101602, http://dx.doi.org/10.1103/PhysRevAccelBeams.25.101602.

[10] P. Muggli, for the AWAKE Collaboration, Physics to plan AWAKE run 2, in: Journal of Physics: Conference Series, Vol. 1596, IOP Publishing, 2020, 012008.

[11] E. Gschwendtner, for the AWAKE Collaboration, AWAKE run 2 at CERN, in: Proc. of IPAC '21, Campinas, Brazil, 2021.

[12] L. Verra, et al., (AWAKE Collaboration), Controlled growth of the self-modulation of a relativistic proton bunch in plasma, Phys. Rev. Lett. 129 (2) (2022) 024802.

[13] A. Caldwell, K.V. Lotov, Plasma wakefield acceleration with a modulated proton bunch, Phys. Plasmas 18 (10) (2011) 103101.

[14] A.A. Gorn, P.V. Tuev, A.V. Petrenko, A.P. Sosedkin, K.V. Lotov, Response of narrow cylindrical plasmas to dense charged particle beams, Phys. Plasmas 25 (6) (2018) 063108.

[15] E. Adli, (AWAKE Collaboration), Towards AWAKE applications: Electron beam acceleration in a proton driven plasma wake, in: Proc. of IPAC '16, Busan, Korea, 2021.

[16] J. Farmer, L. Liang, R. Ramjiawan, F.M. Velotti, M. Weidl, E. Gschwendtner, P. Muggli, Injection Tolerances for AWAKE Run 2c, Technical Report, 2022, arXiv:2203.11622, URL https://cds.cern.ch/record/2806339.

[17] V.K. Berglyd Olsen, E. Adli, P. Muggli, Emittance preservation of an electron beam in a loaded quasilinear plasma wakefield, Phys. Rev. Accel. Beams 21 (1) (2018) 011301.

[18] MAD-X, 2021, http://mad.web.cern.ch/mad/.

[19] R. Ramjiawan, et al., Design of the proton and electron transfer lines for AWAKE run 2c, in: Proc. of IPAC '21, Campinas, Brazil, 2022.

[20] V. Hafych, et al., Analysis of proton bunch parameters in the AWAKE experiment, 2021, arXiv preprint arXiv:2109.12893.

[21] D. Gamba, R. Tomas Garcia, M. Giovannozzi, R. De Maria, J.M. Coello De Portugal-Martinez Vazquez, G. Arduini, M. Cerqueira Bastos, M. Martino, Beam Dynamics Requirements for HL–LHC Electrical Circuits, Technical Report, 2017.

[22] K. Pepitone, S. Doebert, R. Apsimon, J. Bauche, M. Bernardini, C. Bracco, G. Burt, A. Chauchet, E. Chevallay, N. Chritin, et al., The electron accelerators for the AWAKE experiment at CERN—baseline and future developments, Nucl. Instrum. Methods A 909 (2018) 102–106.

[23] E. Forest, F. Schmidt, E. McIntosh, Introduction to the Polymorphic Tracking Code, KEK Report 3, 2002.

[24] M.J. Powell, The BOBYQA Algorithm for Bound Constrained Optimization Without Derivatives, Cambridge NA Report NA2009/06, University of Cambridge, Cambridge, 2009, pp. 26–46.

[25] OCELOT documentation, 2021, URL https://ocelot-collab-docu.readthedocs.io/en/latest/.

[26] L. Verra, E. Gschwendtner, P. Muggli, Study of external electron beam injection into proton driven plasma wakefields for AWAKE Run2, in: Proc. of Journal of Physics: Conference Series, Vol. 1596, IOP Publishing, 2020, 012007.

[27] D.E. Groom, S. Klein, Passage of particles through matter, Eur. Phys. J. C-Particles and Fields 15 (1) (2000) 163–173.

[28] M.B. Reid, Electron beam emittance growth in thin foils: A betatron function analysis, J. Appl. Phys. 70 (11) (1991) 7185–7187.